https://doi.org/10.5194/egusphere-2025-6287
Preprint. Discussion started: 23 January 2026

Sodium Thiosulfate-Coated Ceramic Denuders for Ozone Removal in Ultrafine Particle Sampling

Elisabeth Eckenberger[1], Andreas Mittereder[2], Nadine Gawlitta[3,4], Martin Sklorz[3,4], Dieter Brüggemann[2], Ralf Zimmermann[3,4], Anke C. Nölscher[1*]

[1] Bayreuth Center of Ecology and Environmental Research (BayCEER), University of Bayreuth, Germany

[2] Department of Engineering Thermodynamics and Transport Processes, University of Bayreuth, Bayreuth, Germany

[3] Joint Mass Spectrometry Centre (JMSC) at Comprehensive Molecular Analytics, Helmholtz Zentrum München, Neuherberg, Germany

[4] JMSC at Chair of Analytical Chemistry, Institute of Chemistry, University of Rostock, Rostock, Germany

* now at: Institute of Climate and Energy Systems - Troposphere (ICE-3), Forschungszentrum Jülich GmbH, Jülich, Germany, and Institute of Geophysics and Meteorology, University of Cologne, Cologne, Germany

Correspondence to: Elisabeth Eckenberger (Elisabeth.eckenberger@uni-bayreuth.de), Anke C. Nölscher (a.noelscher@fz-juelich.de)

Abstract. Ozone (O_3) remaining in sampling air can artefactually alter the chemical composition of collected ultrafine particles (UFP), biasing quantitative analysis of the chemical composition. In this study, we developed and evaluated a sodium-thiosulfate O_3 denuder (TSOD) specifically tailored for UFP sampling and assessed its O_3 scrubbing efficiency, particle losses, and chemical selectivity. In laboratory tests under controlled relative humidity and inlet O_3 levels up to 200 ppbV, the outlet concentration remained consistently between 0 and 0.3 ppbV, demonstrating the O_3 removal efficiency of the TSOD. During an urban field deployment over 7 days O_3 downstream of the TSOD consistently remained at 0 ppbV while ambient O_3 varied between 0 and 65 ppbV. Moreover, for particles with mobility diameters ranging from 10 to 1000 nm, we did not observe any significant losses in particle number concentrations. Using a parallel two-channel UFP sampler (with vs. without upstream TSOD), we quantified O_3-driven sampling artefacts in UFP mass focussing on three types of organic markers. (1) Firstly, we targeted polycyclic aromatic hydrocarbons (PAHs), particularly chrysene (Chry), benz[a]anthracene (BaA), benzo[a]pyrene (BaP), indeno[1,2,3-cd]pyrene (IcdP), benzo[k]fluoranthene (BkF), and benzo[b]fluoranthene (BbF). Without upstream O_3 removal, the individual concentration of the PAHs were 15–46% lower. (2) Secondly, for the tire and road wear marker, the antioxidant N-(1,3-dimethylbutyl)-N′-phenyl-p-phenylenediamine (6PPD) and its oxidation product 6PPD-quinone (6PPDq), we observed in-situ ozonation of 6PPD to 6PPDq with transformation yields of about 13 to 20 %. (3) In contrast, biogenic organic acids (bOAs) did not show differences when sampled with or without O_3, as their O_3 reactivity is much lower than the one of the PAHs. Moreover, this test indicated that the TSOD did not perturb the gas–particle partitioning of these semi-volatile species. Our results demonstrate that the TSOD (i) efficiently scrubs atmospheric O_3 at relevant mixing ratios, (ii) does not introduce measurable particle losses across 10–1000 nm, and (iii) preserves semi-volatile partitioning.

https://doi.org/10.5194/egusphere-2025-6287
Preprint. Discussion started: 23 January 2026

1 Introduction

Tropospheric ozone (O_3) is ubiquitous and highly reactive. Close to the Earth's surface, O_3 typically exhibits mixing ratios of up to 80 ppbV, occasionally exceeding 90 ppbV during strong photochemical episodes (Gaudel et al., 2018; Monks et al., 2015). Its tropospheric lifetime is on the order of days to weeks, typically 6–27 days depending on altitude and chemical environment (Prather & Zhu, 2024; Young et al., 2013). O_3 can damage leaf tissues, irritate eyes, and harm the respiratory system, making it an air pollutant with short and long-term effects on ecosystems and human health (Emberson, 2020; Zhang et al., 2019). In the atmosphere, O_3 reacts with a wide range of atmospheric organic compounds. While being an important oxidant and initiating the oxidative removal of unsaturated organic gaseous molecules, O_3 poses a challenge in sampling when these O_3-reactive molecules are targeted in the chemical analysis (Ernle et al., 2023; Monks et al., 2015). If O_3 remains in the sampling air, it can continue to react with other atmospheric compounds bearing O_3-reactive unsaturated functional groups during the collection, thus leading to sampling artefacts. Such O_3-induced artefacts have been long recognized in atmospheric science and especially aerosol sampling (Balducci et al., 2018; Grosjean, 1992; Van Vaeck & Van Cauwenberghe, 1984). In filter-based aerosol samplers, particles often reside on filters from several hours up to several days, providing enough time to react with O_3 of the sampling air streaming through filters and already collected particles. Consequently, collected particles may undergo oxidative reactions with O_3, resulting in distortion of their chemical composition.

To mitigate O_3-induced sampling artefacts, upstream O_3 denuders or scrubbers are recommended for the sampling of particulate matter (e.g. PM2.5 and PM10) by regulatory standards such as CEN EN 15549:2008. Particularly for O_3-reactive species like PAH (European Committee for Standardization (CEN), 2008), those denuders are used to remove O_3 from the sampling air stream and thereby prevent O_3 induced reactions on the filters before analysis.
Most O_3 mitigation concepts were initially developed for gas-phase VOC sampling. Helmig (1997) summarizes the underlying technical principles. These include stoichiometric chemical scrubbers, catalytic decomposition surfaces, and adsorptive traps. However, this study also highlights the key constraint that efficient O_3 removal must be balanced against analyte losses, co-removal of trace gases, or unintentionally induced side reactions with the scrubber. For sesquiterpenes, Pollmann et al. (2005) quantify pronounced O_3-driven sampling losses under atmospherically relevant concentrations, but also show that that mitigation itself can become a source of artefacts.
There are different approaches to remove O_3 upstream of aerosol and gas-phase sampling systems, ranging from physical/thermal decomposition to reactive denuder materials (Fick et al., 2001). One physical approach is the use of heated stainless-steel tubes, which are optimized to thermally decompose O_3. They were shown to improve the sampling of reactive terpenes during ambient measurements, while minimizing additional chemical interferences compared to reactive scrubbers (Hellén et al., 2012). In addition, Koppmann et al. (1995), demonstrate that O_3 can affect cryogenic/thermal-desorption preconcentration itself highlighting the need for explicit upstream O_3 control in such methods. Common approaches include potassium iodide (KI) coatings, manganese dioxide (MnO_2) catalysts, activated carbon (charcoal) adsorbents, silver-coated

https://doi.org/10.5194/egusphere-2025-6287
Preprint. Discussion started: 23 January 2026

surfaces, and sodium thiosulfate ($Na_2S_2O_3$) impregnation (Ernle et al., 2023; Fick et al., 2001; K. Liu et al., 2014; Williams & Grosjean, 1990).

KI based denuders remove O_3 via stoichiometric redox reactions, thereby iodide oxidation products are generated. But the release of those reactive by-products such as I_2 and OH^-, could interact with the atmospheric samples. For example, iodinated compounds and hydroxide from KI based O_3 scrubbers have been shown to degrade derivatization agents that might be used during the extraction procedure, and introduce secondary artefacts in sampling of carbonylic compounds (Ho et al., 2013). MnO_2-coated denuders function via catalytically O_3 removal and have proven to prevent O_3 induced reactions of organic marker compounds in particulate matter. Yet, studies showed, that the strong oxidizing surface of the MnO_2 coated denuders itself can react with components of the sampling air. In particular, while the use of a MnO_2 denuder prevented the loss of particle-bound PAH during sampling, it also led to degradation of some PAH and concurrent formation of oxygenated PAH on the denuder surface (Y. Liu et al., 2006). Activated carbon and silver traps offer broad O_3 removal through adsorption or catalysis, but these materials are relatively non-selective and thus may adsorb other gas-phase species or alter trace constituents in the sampling air (Fick et al., 2001; Liffick, 1970). In contrast, $Na_2S_2O_3$ offers a well-characterized stoichiometric reaction with O_3 yielding in unreactive inorganic products.

Thiosulfate reacts with O_3 via stepwise oxidation, yielding tetrathionate and, under excess O_3, sulfate as stable products. The reaction effectively removes O_3 without generating gaseous radical by-products (equation 1, Takizawa et al., 1973):

$$O_3 + H_2O + 2Na_2S_2O_3 \rightarrow O_2 + 2NaOH + Na_2S_4O_6 \qquad (1)$$

$$Na_2S_2O_3 + 2NaOH + 4O_3 \rightarrow 2Na_2SO_4 + H_2O + 4O_2$$

$Na_2S_2O_3$ coated denuders (TSOD) have been successfully employed in gas-phase sampling to protect analytes (e.g. volatile organic compounds, VOC, such as terpenoids and carbonyls) from O_3 reactions. Practical field implementations further demonstrate the applicability of $Na_2S_2O_3$ -based O_3 removal in gas-phase research. Bouvier-Brown et al. (2009) deployed a TSOD upstream of a GC-system during ambient measurements to suppress inlet/preconcentration ozonolysis and thereby improve the quantification of highly reactive mono- and sesquiterpenes. In one comparative study, both KI and $Na_2S_2O_3$ O_3 filters achieved >90% removal efficiency for about 50 ppbV O_3, although KI showed slightly higher performance and less humidity sensitivity. For $Na_2S_2O_3$, O_3 removal increases with relative humidity (rH) and declines in very dry air, while robust elimination is obtained at ~50–80% rH (Rynek et al., 2025). Crucially, unlike KI, the thiosulfate method does not introduce organic reactive by-products, offering a potential advantage for preserving the organic composition of particle samples (Fick et al., 2001). Despite that, sodium thiosulfate O_3 denuders have seen little application in particulate-matter sampling compared with established O_3-denuders to date, and their performance in that context remains largely unexplored.

https://doi.org/10.5194/egusphere-2025-6287
Preprint. Discussion started: 23 January 2026

This knowledge gap is particularly relevant for ultrafine particles (UFPs, diameter < 100 nm), which are of special interest due to their many, diverse sources and health implications (Balmes & Hansel, 2024; Haddad et al., 2024; Li et al., 2023; Marval & Tronville, 2022). Among others, UFP distinguish from coarser particles because of their small mass, high number concentration and high surface-area-to-mass ratio and high diffusional mobility. Thus, UFPs can readily adsorb gases, like O_3 and other oxidants, and undergo rapid surface chemistry. These properties not only facilitate heterogeneous reactions, altering particle composition, but also influences toxicological behaviour (Kwon et al., 2020; Oberdörster et al., 1992).

A particularly relevant example is the enrichment of polycyclic aromatic hydrocarbons (PAH) in UFP. PAH are ubiquitous environmental pollutants originating from anthropogenic activities such as biomass burning and fossil fuel combustion (Abdel-Shafy & Mansour, 2016). They are of concern due to their persistence, potential for long-range transport, and the formation of toxic transformation products in the atmosphere (Ravindra et al., 2008). Their atmospheric lifetime and toxicity profiles are governed by multiphase oxidation pathways involving gas-phase radicals and O_3. Among others, the higher-molecular-weight PAH (≥5 rings; benzo[a]pyrene (BaP), benzo[b]fluoranthene (BbF), benzo[k]fluoranthene (BkF), indeno[1,2,3-cd]pyrene (IcdP), together with four-ring PAHs such as chrysene (Chry) and benz[a]anthracene (BaA), are known to undergo heterogeneous ozonolysis on particle surfaces, especially under conditions of elevated O_3 exposure (Ji et al., 2024).

Another prominent example is N-(1,3-dimethylbutyl)-N′-phenyl-p-phenylenediamine (6PPD), a widely used tire antiozonant that protects rubber surfaces through reactive scavenging of O_3. During tire wear, 6PPD is released into the environment and oxidized via O_3 to 6PPD-quinone (6PPDq). This transformation product has recently shown to exhibit acute aquatic toxicity, particularly toward coho salmon (Hu et al., 2022 ; H. N. Zhao et al., 2023).

A further compound class of interest are biogenic organic acids (bOAs), secondary oxidation products of monoterpenes that serve as markers for biogenic secondary organic aerosol (SOA) formation and ageing (Christoffersen et al., 1998; et al., 1998; Denjean et al., 2015; Mutzel et al., 2016). This includes pinic acid (PA), pinonic acid (POA), terpenylic acid (TPA), and terebic acid (TA), which span a broad range of volatility: while PA is mainly particle-bound, POA, TPA, and TA remain partly in the gas phase (Kristensen, Bilde, et al., 2016; Yu et al., 1999). Because of their semi-volatile nature, non-specific adsorption of gas-phase bOAs or disturbance of the gas–particle equilibrium are known artefact pathways in denuder-based sampling**,** which can alter the measured particle-phase concentrations (Subramanian et al., 2004; Yatavelli et al., 2014;Yatavelli et al., 2012). This issue is particularly relevant for UFP sampling, where the high surface-area-to-mass ratio enhances adsorption and desorption processes and thus amplifies potential denuder artefacts (Kristensen, Watne, et al., 2016; Kuwabara et al., 2016; Shiraiwa et al., 2011).

Given the emerging significance of UFP as important contributors to air pollution in atmospheric chemistry and human health, being linked to oxidative stress, respiratory and cardiovascular diseases (Das et al., 2024; Pantzke et al., 2023), such artefacts can bias the interpretation of UFP chemical composition and reactivity, underscoring the need for artefact-free sampling when assessing their environmental and health relevance (Schraufnagel, 2020).

https://doi.org/10.5194/egusphere-2025-6287
Preprint. Discussion started: 23 January 2026

To address this, we designed a study combining laboratory and field experiments to assess the performance of TSOD for UFP composition analysis under controlled and ambient conditions. Specifically, we focused on three representative classes of marker compounds: (1) PAHs to quantify O_3-induced losses; (2) tire-derived N-(1,3-dimethylbutyl)-N′-phenyl-p-phenylenediamine (6PPD) and its quinone (6PPDq) as a parent–product pair indicative of in-sampler ozonation; and (3) biogenic organic acids (bOAs) to test the selectivity and potential disturbance of gas–particle equilibrium.

2. Methods

2.1. O_3 denuder preparation

As O_3 denuder body, we used ceramic bodies (Ø 25.4 x 50 mm; squared channels with 400 CPSI, Rauschert, Germany) that were impregnated with $Na_2S_2O_3$ (Merck, 99%). Before coating the ceramic bodies, they were heated to 500 °C for 5 h, then cleaned in water (H_2O, obtained from Seralpur PRO 90 CN system with Supor DCF filter, Electronics Grade, 0.2 µm), subjecting them to ultrasonication for two cycles, each for 10 minutes. Subsequently, the bodies were manually dried with vigorous shaking to ensure the complete removal of water. Next, the bodies were placed in a 5,6 mol L^{-1} solution of $Na_2S_2O_3$ and H_2O, and ultrasonicated for an additional 10 minutes. It was imperative to thoroughly dry the denuders again with shaking and blow-drying it with nitrogen (N_2, 99.99%). This was a critical step to prevent the growth of crystals within the ceramic matrix and the subsequent occlusion of the channels. The drying process was finished by baking the TSODs at a temperature of 120°C for a duration of 60 minutes. For storage, the TSODs were placed in a sealed container with a separate water reservoir at the base to maintain a high humidity environment. This setup was left to rest overnight, for 12 hours, to achieve an even coating of $Na_2S_4O_3$ on the ceramic body. Afterwards the TSODs were stored under N_2 atmosphere in a closed glas vessel.

2.2 Laboratory test-bed for determining the denuder efficiency for O_3 removal under controlled conditions

To assess the O_3 removal efficiency of the TSODs, we set up an experimental test-bed in the laboratory. O_3 was produced in variable levels with a generator (Teledyne, T750U), diluted with zero air at a flow rate of 4 L min^{-1}, and passed through the TSOD. Upstream of the TSOD, humidified air was added to the sample flow by bubbling 4 L min^{-1} of zero air through a suction flask filled with H_2O, yielding a total flow of 8 L min^{-1} through the TSOD (Fig. 1a). We measured the relative humidity (rH) upstream of the TSOD, which remained constant at about 50%. Downstream of the TSODs, the O_3 mixing ratio was measured using an O_3-analyzer (Thermo Scientific, MLU, Model 49i). We tested the TSOD for a range of O_3 mixing ratios of 5 to 200 ppbV.

2.3 Assessment of particle losses within the O_3 denuder

To examine potential particle losses due to the TSOD, we conducted loss tests with simulated atmospheric organic aerosol (SimOA) using the Bayreuth Atmospheric simulation Chambers (BATCH). To maintain a stable aerosol mixture for several hours, we flushed the 700L cylindrical glass chamber with ambient air for several hours. Subsequently, 0.05 mL of alpha-pinene (≥98,0 %, Carl Roth) was injected into the airflow, while a nebulizer delivered seed particles (from spraying saturated

https://doi.org/10.5194/egusphere-2025-6287
Preprint. Discussion started: 23 January 2026

ammonium sulfate solution and drying) into the chamber at a flow rate of 3 L min⁻¹ for 3 minutes. After an additional 5 minutes, the pump supplying ambient air was switched off, and the solar simulator (UV Osram HMI, 4000 W, filtered with a water-cooled glass plate) (Ofner et al., 2011; Z. Zhao et al., 2008), was ignited for 15 minutes to produce first O_3 and subsequently SimOA. We connected three TSOD bodies in line to the chamber. Downstream the TSOD, a Y-connector was attached splitting the flow into two channels. One channel end led to a pump which allowed to adjust to variable flows through the denuder (4-30 L min⁻¹). The other channel end led to a particle size spectrometer to record the particle size distribution after the TSOD (Cambustion, DMS500). As a control, the setup was also operated without the TSOD installed in the stainless-steel cylinders.

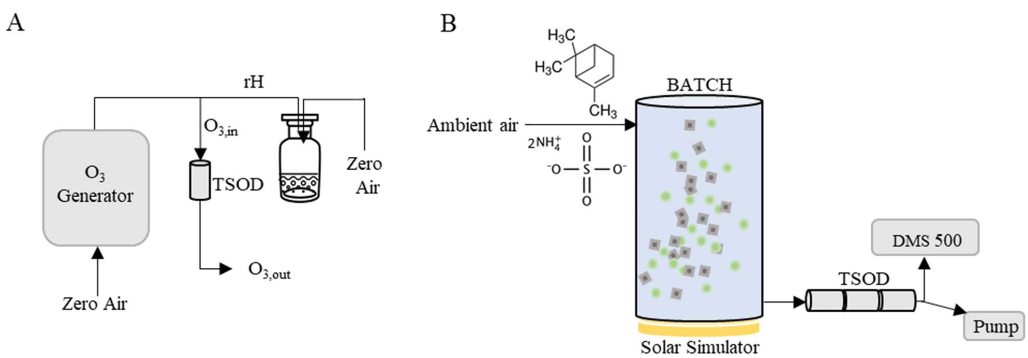

Figure 1 Schematic of the laboratory test-bed for assessing the O_3 removal efficiency (A) and potential particle losses of TSODs (B). (A) O_3 was generated, diluted with zero air, humidified to ~50% relative humidity, and passed through the TSOD. Downstream O_3 concentrations were measured using an O_3 analyzer. (B) For particle loss tests, the setup was connected to the BATCH, where SimOA was generated from α-pinene oxidation with ammonium sulfate seed particles and ambient air. The aerosol flow was directed through three TSODs, and particle size distributions were measured downstream using a DMS500.

2.4 Field deployment and UFP sampling for offline chemical characterization

To evaluate the performance of the TSOD under real environmental conditions, a novel setup was installed in a measurement container at an urban field site of the University of Applied Sciences in Augsburg, Germany (48.357947° N, 10.907090° E) in September 2023. The site is dominated by domestic heating and traffic which are a likely sources for PAH and 6PPD/6PPDq. Streetside and campus vegetation emitted monoterpenes, providing biogenic precursors for SOA. Air was drawn through a PM10 sample inlet from the roof of the air-conditioned container at a height of 4.2 m. A stainless-steel sampling tube (2.1 m x 28 mm) led into the container, where it was connected to a modified 120 R Microorifice Uniform Deposit Impactor (MOUDI, TSI). The 120R-MOUDI was reduced to sample with cut-off sizes of 2.5, 1.0, and 0.1 µm. The impactor plates were coated with high-vacuum grease to minimize bounce effects. Behind the reduced MOUDI unit, the After Filter Stage, intended to collect particles smaller than 0.1 µm, was omitted, and instead, a Y-connector (30 cm x 28 mm) was installed, leading to an

https://doi.org/10.5194/egusphere-2025-6287
Preprint. Discussion started: 23 January 2026

automated filter changer (HYDRA Dual Sampler, FAI instruments), thereby introducing a two-channel filter collector. Here, UFP samples were collected from both channels in parallel on pre-baked quartz fiber filters (47mm Whatman, QM-A) and, following a weekly change, stored at -20°C in analyslides (Cytiva) until analysis. In one of these channels (Channel A), the TSOD was installed, while the other channel (Channel B) was operated with an uncoated ceramic body as reference. For control measurements, both channels were operated with a ceramic body without coating. The total flow through the impactor was set to 30 L min^{-1} according to the manufacturer's specifications, with a corresponding collection of 15 L min^{-1} per channel. Ambient O_3 concentrations were measured after channel A (41M, UV Photometric O_3 analyzer, ansyco, environment s.a) and cross-checked against values reported by the local governmental monitoring station (Landesamt für Umwelt, LfU). This field setup intended to serve: (i) as assessment of the O_3 removal efficiency under real-world conditions over a longer time period, and (ii) the effect of O_3 removal during collection of UFP samples for subsequent offline chemical analysis.

2.5 Chemical marker compounds

UFP samples obtained during the field campaign were analyzed offline to investigate the effect of upstream O_3 removal via TSOD on the concentrations of selected organic marker compounds. The following target compounds were analyzed: (i) PAHs: BaP, BbF, Bk, IcdP, Chry, and BaA; (ii) parent–product (ozonolysis) pair: 6PPD and 6PPDq; and (iii) bOAs: PA, POA, TPA, and TA. Internal standards were 3-methylcholanthrene (3-MC, Merck, 98.0 %, 0.4 µM) and nicotinic acid (NA, Merck, 99.5%, 10 µM). Reagents, solvents, and standards were sourced from LGC Standards, Merck, Carl Roth, ASCA-Berlin, and Fisher Chemical (purities >95–99.99 %). HPLC-grade acetonitrile (ACN, 99.95 %), methanol (MeOH, 99.99 %), water (H_2O; Seralpur PRO 90 CN, electronics grade, 0.2 µm), and formic acid (HCOOH, ≥98%) were used as mobile-phase components; dichloromethane (DCM, 99.8 %) and high-purity nitrogen (N_2, 99.999 %) were used for extraction/solvent handling and evaporation.

2.6 Extraction

The methodology for filter extraction has been described by Eckenberger et al. (2025). Briefly, we extracted the selected marker components from the filters via a soft, solvent-based and optimized protocol: (1) the filter loaded with particles was divided into two equal parts. One part was extracted, the other one used as backup. (2) The filter-half for extraction, was spiked with 50 µL of each internal standard, namely 3-methylcholanthrene (3-MC, 0.4 µM) and Nicotinic acid (NA, 10 µM) and cut into small fragments. (3) These filter fragments were then transferred into a glass container with a screw cap, and 2 mL of extraction solvent (e.g. analytical-grade dichloromethane (DCM, Fisher Chemical, 99.8%) and methanol (MeOH, Carl Roth, ≥ 99.9%)) were introduced. (4) The samples underwent extraction through agitation within a closed flask for a duration of 15 minutes using a vortex shaker (2000 rpm). (5) Filter residues were kept in the glass container. Extracts were filtered using custom-designed glass frits with a diameter of 1 cm and a pore size of 20 µm to filter any potential filter residue.

https://doi.org/10.5194/egusphere-2025-6287
Preprint. Discussion started: 23 January 2026

Steps (3) to (5) were repeated three times, each time employing a different extraction solvent. The sequential solvents used were, in order, pure MeOH, 50:50 MeOH:DCM, and pure DCM. Subsequently, the solvent from the combined extracts was evaporated under a gentle flow of nitrogen while cooled with ice to avoid loss of semi-volatile compounds. A droplet was kept as residue which was dissolved in 1 mL of a 60:40 solution of acetonitrile (ACN, Carl Roth, 99.95%) and Millipore water (H_2O obtained from Seralpur PRO 90 CN system with Supor DCF filter, Electronics Grade, 0.2 µm). This was transferred into two separate vials for subsequent analysis. Throughout this entire sample preparation process, the samples were consistently stored in an ice cooled environment to avoid losses.

2.7 HPLC methods

The extracts of the collected UFP were analyzed using two complementary high-performance liquid chromatography (HPLC) systems, adapted to the specific analytical requirements of the target compounds. PAHs were quantified using an Agilent 1260 Infinity system equipped with a fluorescence detector (Agilent 1100 Series FLD). bOAs and tire-derived antioxidants, including 6PPD and its transformation product 6PPDq, were analyzed on an Agilent 1100 Series HPLC coupled to an electrospray ionization mass spectrometer (ESI-MS; Agilent 6130 Single Quadrupole).
All analyses were conducted using HPLC-grade solvents: acetonitrile, ultrapure water, and formic acid (≥98 %, Carl Roth). Chromatographic separation and detection settings were optimized for each compound class. A detailed summary of the applied methods is provided in our previous publication and in the SI (Eckenberger et al., 2025; Table S1).
To assess the overall analytical recovery, spiking experiments were performed in triplicate. One half of a pre-baked quartz fiber filter (47 mm, Whatman QM-H) was spiked with 10 µL of a 10 µM standard solution containing all target compounds and subsequently extracted following the same procedure used for ambient samples. Recoveries were calculated using external calibration and expressed as the ratio of measured to expected concentrations:

$$Rec = \frac{c_{measured}}{c_{expected}} \times 100 \qquad (2)$$

Average recoveries ranged from 70 % to 101 % and were consistent across compound classes. Specifically, recoveries for PAHs were 78 ± 5 % for BaP, 74 ± 4 % for BbF, 89 ± 6 % for BkF, 70 ± 4 % for IcdP, and 97 ± 5 % for ΣChry+BaA. 6PPD and its transformation product 6PPDq yielded recoveries of 75 ± 7 % and 81 ± 7 %, respectively. Among the bOAs, PA was recovered at 84 ± 6 %, while POA, TA, and TPA showed recoveries of 101 ± 6 %, 85 ± 6 %, and 96 ± 6 %, respectively.

To account for analyte-specific losses, all sample concentrations were corrected for recovery using the following equation:

$$c_{sample_{corrected}} = c_{sample_{measured}} \times \left(\frac{100}{Rec}\right) \qquad (3)$$

https://doi.org/10.5194/egusphere-2025-6287
Preprint. Discussion started: 23 January 2026

Validation of the analytical procedure was performed using the NIST Standard Reference Material SRM 2786 (Fine Atmospheric Particulate matter with mean diameter <4 µm), which was applied to a quartz filter and processed identically to the environmental samples. The results agreed with the certified concentrations within their stated uncertainty, confirming the reliability of the method even in the presence of a complex particulate matrix. Limits of detection (LOD) were determined for each compound from four replicate injections of a diluted calibration standard, targeting a signal-to-noise ratio of 3. The LOD was calculated as:

$$LOD = \frac{3\times\sigma}{RF} \tag{4}$$

where σ is the standard deviation of replicate peak areas and RF denotes the compound-specific response factor derived from external calibration. For comparison with ambient concentrations, airborne detection limits LOD_{Air} were calculated by normalizing the LOD to the sampling volume (Table S2).

Instrument and field blanks were routinely collected and processed alongside samples using the identical preparation. Instrument blanks consisted of pure-solvent injections between runs. Field filter blanks were prepared by placing clean quartz filters in the sampler holders but without drawing air. Blank signals were subtracted on a per-compound basis when reproducible across replicate blanks and clearly below sample signals. If blank values varied strongly within a batch or exceeded expected background levels, affected samples were excluded from further analysis.
Last step to calculate mass concentrations of the marker compounds in UFP was to convert the blank-corrected extract concentrations to air concentrations by multiplying the corrected concentration by the final extract volume (1 mL), correcting for recovery and the analyzed filter fraction (only half filter was analyzed), and normalizing to the sampled air volume (21.6 m³).

3. Results and Discussion

3.1 Laboratory evaluation of denuder performance

To evaluate the O_3 removal efficiency of the TSOD under controlled conditions, we first conducted a laboratory test. Previous studies have shown that rH plays a critical role in the reactivity of sodium thiosulfate toward O_3 (Ernle et al., 2023). Specifically, at 80% rH, the lifetime of the sodium thiosulfate scrubber increases dramatically, enabling complete O_3 removal from the sample air, in contrast to its performance under dry conditions. As a reference for typical ambient conditions at our field site in Augsburg, daily data from the nearest German Weather Service (Deutscher Wetterdienst, DWD) climate station for the meteorological summer 2023 yield an average relative humidity of 69 % ± 11 % (Data source: DWD). We therefore intentionally conducted our laboratory experiments under distinctly drier conditions (rH = 52.4–53.3 %), in order to test TSOD performance near the lower end of the humidity range expected during field operation, where the scrubber is known to be less

https://doi.org/10.5194/egusphere-2025-6287
Preprint. Discussion started: 23 January 2026

efficient. In urban and suburban environments, O_3 levels frequently peak between 70 to 100 ppbV and can surpass 120 ppbV during intense pollution events (Bell et al., 2007; Cooper et al., 2014; WHO, 2021). Thus, the inlet O_3 mixing ratio was incrementally increased to up to 200 ppbV. As depicted in Figure 2, the outlet O_3 mixing ratio remained consistently between 0 and 0.3 ppbV.

This indicates that, even at comparably high mixing ratios, O_3 was removed from the air in this experimental setup. However, it is important to note that this experiment was conducted under controlled laboratory conditions with constant temperatures, rH, and zero air. Furthermore, the duration of the experiment does not match the typical collection duration required for UFP, which, due to their low mass, must be collected over several hours or days for mass-based chemical analysis. To complement the controlled laboratory evaluation, a field deployment was conducted to assess the TSOD's applicability under real-world sampling conditions. The results of this field implementation, including performance under ambient O_3 exposure and implications for UFP sampling, are discussed in detail in Section 3.2.

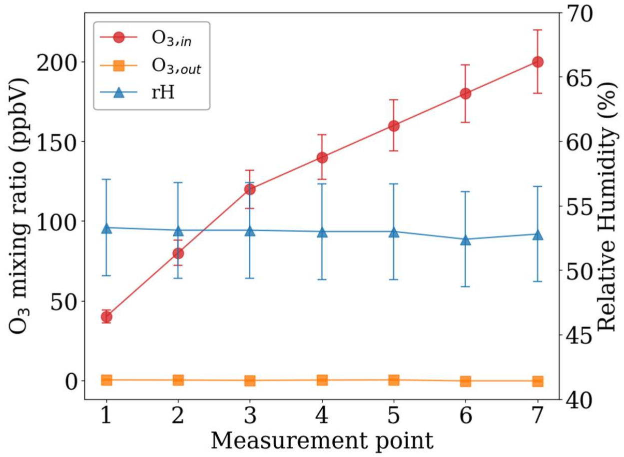

Figure 2 Average O_3 mixing ratios upstream ("O_3 In", red) and downstream ("O_3 Out", orange) of the TSOD under controlled laboratory conditions for varying inlet O_3 mixing ratios (40–200 ppbV). Relative humidity (rH) was simultaneously monitored and remained constant. Lines are included to guide the eye.

To assess if the sampling flow channelled through the TSOD is associated with particle losses, we compared particle number concentrations (PNC) measured with (wTSOD) and without (woTSOD) TSOD installed, where the woTSOD setup served as the reference using an empty TSOD housing. The analysis was performed for two particle size ranges: 10–100 nm and 10–1000 nm. All measurements were repeated at three flow rates (4, 11, and 30 L min^{-1}), and an instrument uncertainty of 10 % was assumed. In the 10–100 nm range, relative differences between the wTSOD and woTSOD configurations ranged from 2 % to 7 % depending on the flow rate. At 4 L min^{-1}, the difference corresponded to a 2 % loss, increasing to 7 %, and 6 % at 11 L min^{-1} and 30 L min^{-1}, respectively.

https://doi.org/10.5194/egusphere-2025-6287
Preprint. Discussion started: 23 January 2026

Comparable results were obtained for the full-size spectrum (10–1000 nm). Measured losses amounted to 7 % (4 L min^{-1}), 3 % (11 L min^{-1}), and 6 % (30 L min^{-1}) (Fig. 3).

The average observed deviation between the wTSOD and woTSOD measurements was 5% and falls within the measurement uncertainty of the particle size spectrometer utilized. Hence, we found no significant losses in particle number concentrations and the TSOD setup can be considered suitable for ambient UFP sampling.

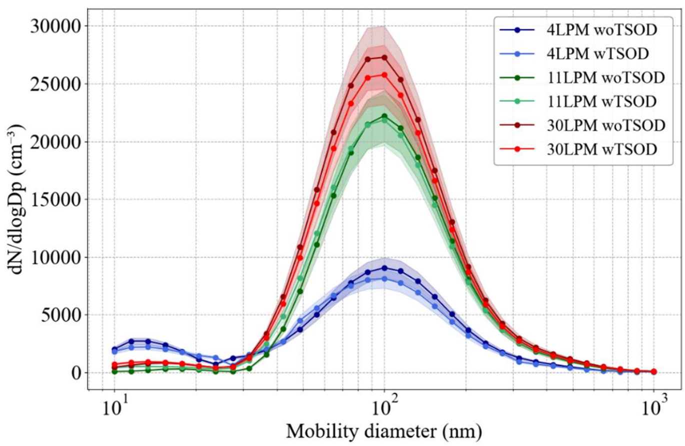

Figure 3 Particle size distributions recorded downstream of the TSOD and for reference without a TSOD at three different flow rates (4, 11, and 30 L min^{-1}). Blue tones refer to 4 L min^{-1} (royal blue: wTSOD, dark blue: woTSOD), green tones to 11 L min^{-1} (Medium Green: wTSOD, dark green: woTSOD), and red tones to 30 L min^{-1} (red: wTSOD, dark red: woTSOD). Shaded areas represent ±10% uncertainty.

3.2 Field performance of the denuder and chemical composition of UFP

The O_3 removal performance of the TSOD was further evaluated under ambient conditions during a five-day deployment at an urban field site. Due to the lack of a second O_3 analyzer, the experiments were conducted using only one device. Initially, measurements were taken with the O_3 analyzer without the installed coated ceramic body. Subsequently, these measurement results were compared with publicly available data on O_3 concentrations from a nearby site monitored by the Bavarian Environment Agency (Bayerisches Landesamt für Umwelt (LfU). LÜB – Messwertarchiv: O_3, hourly data, station Augsburg/LfU, 8th August until 13th September 2023. Accessed 8th June 2025).

The hourly averaged data are compared in Figure 4a. A linear regression yielded a slope of 1.04 and a coefficient of determination (R^2) of 0.90, confirming the comparability of both datasets within the uncertainty of the measurement. Therefore, no correction was applied to either dataset before subsequent analysis.

https://doi.org/10.5194/egusphere-2025-6287
Preprint. Discussion started: 23 January 2026

During the period when a TSOD, in channel A of the measurement setup, was installed, the O_3 mixing ratio behind the TSOD was consistently measured. In comparison to the measurements from the Bavarian Environment Agency, it was observed that the O_3 mixing ratio behind the TSOD remained at 0 ppbV, while the outdoor O_3 mixing ratios fluctuated between 0 and 65 ppbV (Fig 4b). Over the period of 5 days, the TSOD removed O_3 reliably from the sampled air. These results indicate the O_3 removal efficiency of the TSOD under environmental conditions and over an extended time period.

https://doi.org/10.5194/egusphere-2025-6287
Preprint. Discussion started: 23 January 2026

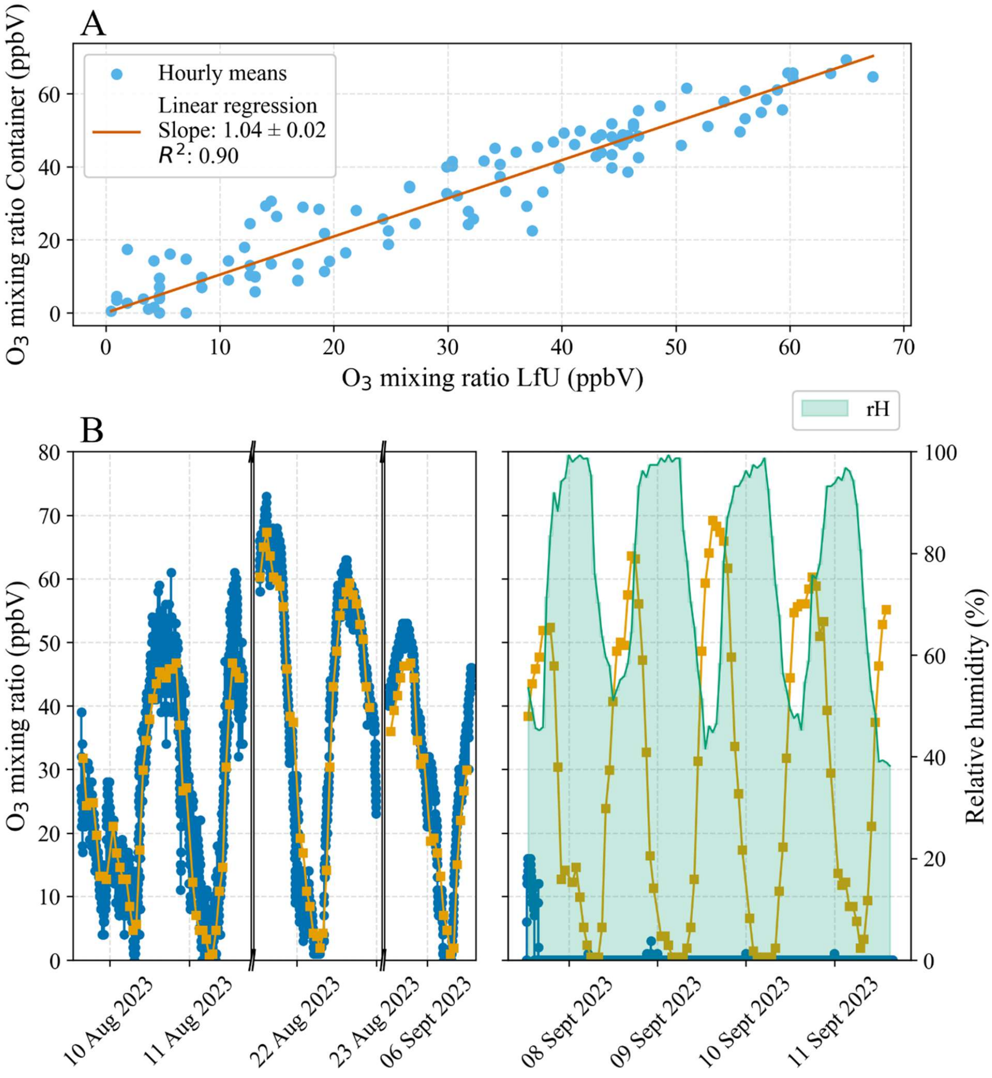

350 **Figure 4 (A) Correlation between hourly averaged O_3 concentrations from the sampling site and the LfU monitoring station. A linear regression through the origin (red line) yields a slope of 1.04 and $R^2 = 0.90$. (B) Time line of ambient O_3 concentrations before and during the field campaign in Augsburg. Measurements before the campaign were taken from a setup without a TSOD, allowing comparison with reference data from the Bavarian Environment Agency. After the start of UFP sampling, measurements were taken downstream of the TSOD (blue, "Sampling site") and compared to the LfU reference data (orange, "LfU").**

https://doi.org/10.5194/egusphere-2025-6287
Preprint. Discussion started: 23 January 2026

3.2.2 Chemical organic tracer analysis of UFP

To assess the efficiency and selectivity of the TSOD under ambient conditions, we evaluated changes in particle-phase concentrations of selected organic tracer compounds. We analyzed representative compounds from three organic marker groups: PAHs, 6PPD and 6PPDq, and bOAs. All compounds are potentially susceptible to TSOD-induced sampling improvements or artefacts. This could be either by prevented degradation through O_3 oxidation or by shifts in gas-particle partitioning through removal of gaseous components. In the following, we present compound-specific mass concentrations measured in Channel A (with O_3 removal via TSOD) and Channel B (without O_3 removal comparing to an uncoated ceramic body). We assess the TSOD performance for each class of marker compounds.

First, to verify the performance and internal consistency of the dual-channel sampling setup, all targeted marker substances were analyzed under reference conditions in which neither sampling line contained an upstream-coated ceramic body. The measured mass concentrations of all compounds in UFP sampled through Channel A and Channel B agreed within the uncertainties. Regression slopes were close to unity for PAHs (BaP: 0.97 ± 0.11, BbF: 1.18 ± 0.13, BkF: 0.83 ± 0.07, IcdP: 1.05 ± 0.16, ΣChry+BaA: 0.92 ± 0.03), demonstrating the absence of systematic differences between the two channels. Similarly, mass concentrations of 6PPD (slope = 1.01 ± 0.04) and 6PPDq (slope = 1.04 ± 0.05) and the bOAs, including PA (slope=1.00 ± 0.01), POA (slope = 1.01 ± 0.02), TA (slope = 1.00 ± 0.02), and TPA (slope = 1.01 ± 0.02) were comparable for both channels (Table 1). Detailed regression plots are provided in the Supporting Information (SI) (Figures S2).

Deploying the TSOD in Channel A and regressing concentrations in Channel B (no O_3 removal) against Channel A provides a direct quantitative analysis of O_3 induced sampling artefacts. For PAHs, slopes of 0.54–0.85 (BaP: 0.60 ± 0.009, BbF: 0.85 ± 0.23, BkF: 0.66 ± 0.14, ΣChry+BaA: 0.54 ± 0.15, IcdP: 0.62 ± 0.17; Table 1) indicate about 15 to 46 % in-sampler losses when O_3 is present (Fig 5a). For context, ambient BaP was on the order of about 9 pg m^{-3} with the deployment of a TSOD, without O_3 removal this would be 40 % lower. In contrast, 6PPD and its oxidation product 6PPDq show opposite behaviour (Fig. 5b, Table 1): 6PPD exhibits a slope of 0.52, indicating underestimation without O_3 removal, whereas 6PPDq shows a slope of 1.40, reflecting overestimation due to in-sampler ozonolysis. These findings are consistent with the oxidative conversion of 6PPD to 6PPDq, which is suppressed in-situ when O_3 is scrubbed from the sampling air. Mechanistic and computational studies have shown that O_3 attacks the aromatic amine moiety of 6PPD, forming hydroxylated intermediates that subsequently oxidize to 6PPDq as the major transformation product (Cataldo, 2019; Rossomme et al., 2023; H. N. Zhao et al., 2023). In our dual-channel approach, we find that about 13 to 20 % of the initial 6PPD was converted to 6PPDq. These transformation yields align with those reported by Zhao et al. (2023), who reported that 1–19 % of 6PPD was converted to 6PPDq during controlled ozonation of 6PPD.

https://doi.org/10.5194/egusphere-2025-6287
Preprint. Discussion started: 23 January 2026

Conversely, bOAs exhibited negligible inter-channel differences (slopes about 1.0 to 1.03, Fig 5c, Table 1), indicating that the TSOD effectively removes O_3 without perturbing gas–particle partitioning. Given their semi-volatile nature, any non-selective uptake or release by the TSOD would shift this equilibrium and drive evaporation or condensation, which is not observed (Kristensen, Bilde, et al., 2016; Yu et al., 1999). This indicates that the sodium thiosulfate coating does not disturb gas-particle equilibrium.

https://doi.org/10.5194/egusphere-2025-6287
Preprint. Discussion started: 23 January 2026

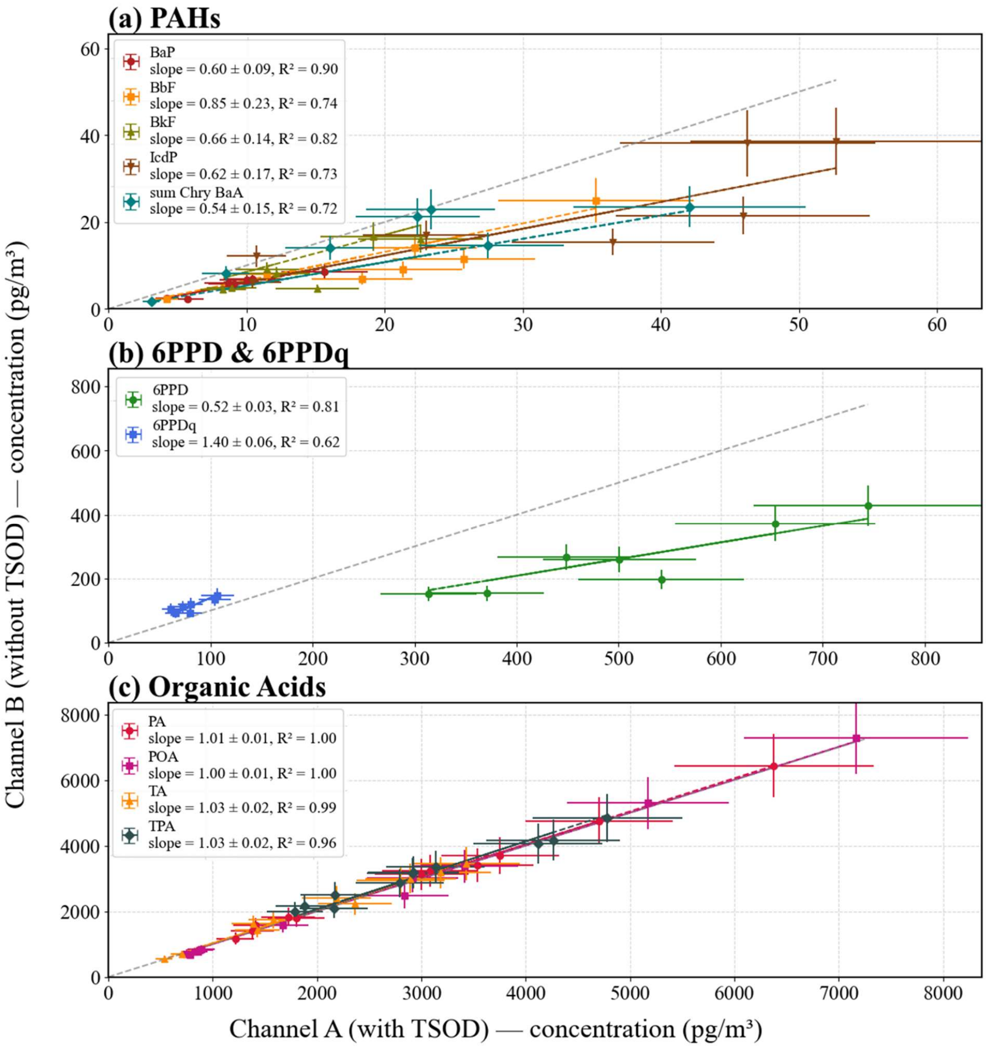

Figure 5 Comparison of analyte concentrations measured in sampling channel A (with TSOD, O_3 removed) and channel B (without TSOD, O_3 present). The sample in channel B was exposed to ambient O_3 mixing ratios during the 24hr sampling interval. Each data point represents the mass concentration of an analyte measured in parallel filters. Dashed lines show linear regressions constrained through the origin, while grey dashed lines represent the 1:1 relationship. (A) PAHs: BaP, BbF, BkF, IcdP, and sum Chry BaA. (B) Tire wear antioxidants and their transformation product: 6PPD and 6PPDq. (C) bOA: PA, POA, TPA, and TA. The standard deviation used for the error bars is derived from three replicate measurements of three extracted filter samples.

https://doi.org/10.5194/egusphere-2025-6287
Preprint. Discussion started: 23 January 2026

Table 1 Linear regression slopes of marker compound concentrations between sampling channels for measurements with and without O_3 removal (reference). Slopes were derived from linear regressions constrained through the origin. Values greater or smaller than unity indicate enhancement or loss of the respective compound in the presence of O_3 removal.

	Slope	
Compound	**Relative change due to O_3 exposure during sampling**	**Reference**
BaP	0.60 ± 0.009	0.97 ± 0.11
BbF	0.85 ± 0.23	1.18 ± 0.13
BkF	0.66 ± 0.14	0.83 ± 0.07
IcdP	0.62 ± 0.17	0.98 ± 0.16
Sum Chry BaA	0.54 ± 0.15	0.92 ± 0.03
PA	1.01 ± 0.01	1.00 ± 0.01
POA	1.00 ± 0.01	1.01 ± 0.02
TA	1.03 ± 0.02	1.00 ± 0.02
TPA	1.03 ± 0.02	1.01 ± 0.02
6PPD	0.52 ± 0.03	1.01 ± 0.04
6PPDq	1.40 ± 0.06	1.04 ± 0.05

Among the PAHs, the most pronounced O_3 related losses were observed for the sum of BaA Chrys (46 %) and for BaP (40 %), followed by IcdP (38 %), BkF (34 %), and BbF (15 %). These losses observed in the UFP fraction are consistent with sampling artefact studies focusing on O_3 related degradation in larger particle fractions.

For PM_{10}, Balducci et al. (2018) reported summer field BaP concentrations of about 0.022 to 0.028 ng m^{-3} and, in laboratory tests at 400 ppbV O_3 for 1–3 h, observed BaP losses of ~24–55% (with smaller losses for BbF and BkF). Similarly, Y. Liu et al. (2006) reported daily O_3 concentrations of 50–95 µg m^{-3} (≈ 25–48 ppbV at 290 K) and deployed a MnO_2 denuder into PM_7 sampling. The observed concentrations for particulate PAH rose from 0.16 to 0.20 ng m^{-3} (+25%) for BaP and shifts for BaA (−7%), chrysene (−14%), and IcdP (+6%), while BbF remained unchanged upon the removal of O_3. Consistently, the study of Liu et al. (2014) in Beijing summer showed averaged O_3 concentrations of 74.6 µg m^{-3} (~37 ppbV). They sampled $PM_{2.5}$ with a denuder-equipped method, which yielded higher particulate PAH concentrations than the conventional setup (Σ_9PAH = 42.3 ± 10.5 vs 27.1 ± 13.8 ng m^{-3}), and for BaP a corresponding underestimation from 49% to 83% without O_3 removal. While inter-channel artifacts such as gas-particle partitioning ("blow-on" or "blow-off") might occur, our control measurements showed no inter-channel bias in the absence of the TSOD. Therefore, we conclude that the observed differences are primarily driven by O_3-induced chemical transformation of particle-bound PAHs in the channel without the denuder.

https://doi.org/10.5194/egusphere-2025-6287
Preprint. Discussion started: 23 January 2026

To contextualize the relative O_3-induced artefacts, we compared them with the heterogeneous pseudo–first-order rate constants (k′) for O_3 loss of particle-bound PAHs reported by Bedjanian & Nguyen, (2010). In this study, soot from a premixed kerosene–air flame was exposed to an initial O_3 of 1.3×10^{12} molecules cm^{-3} (≈ 51.4 ppbV at 290 K) under dry, dark flow conditions. Figure 6 shows that our observed UFP degradation pattern generally follows the compound-specific reactivities described by Bedjanian & Nguyen (2010). Consistently with those compound-specific reactivities, our degradation pattern largely follows Σ(Chry + BaA) > BaP ≳ BkF. Quantitatively, Σ(Chry + BaA) shows the highest k′ (7.3×10^{-3} s^{-1}), followed by BaP (6.8×10^{-3} s^{-1}) and BkF (6.0×10^{-3} s^{-1}). BbF has a comparable k′ (5.5×10^{-3} s^{-1}), about 80% of BaP, yet its O_3-related loss in our data is only ~40% of BaP. This discrepancy likely reflects particle-phase microphysics, specifically the partial embedding or molecular shielding within condensed organic matrices. These structural factors inherently reduce the effective surface accessibility of certain PAHs (Kwamena et al., 2007; Shiraiwa et al., 2011; Zhou et al., 2019). Furthermore, the elevated relative humidity during sampling (74–84 %) may have further enhanced this effect, by increasing particle viscosity or forming hydrated amorphous surface layers which can act as transient diffusion barriers (Pöschl et al., 2001). Consequently, while the relative ranking of O_3 susceptibility among PAHs in UFP is preserved, the overall magnitude of degradation is likely strongly influenced by particle-phase microphysics. This distinction underscores the critical importance of integrating such particle-phase effects when extrapolating laboratory kinetic data to realistic atmospheric conditions.

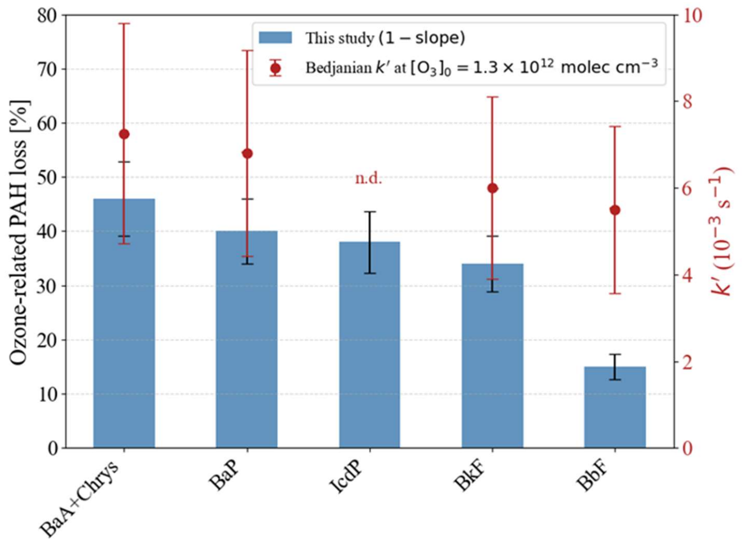

Figure 6 Compound-specific comparison of O_3 induced losses of particle-bound PAH. Blue bars (left axis) show the O_3-attributable loss fraction from this study (1 – slope of the O_3-contrast regression). Red symbols (right axis) show first-order consumption rate constants k′ ($\times 10^{-3}$ s^{-1}) from Bedjanian & Nguyen (2010) for soot exposed to $[O_3]_0 = 1.3 \times 10^{12}$ molec cm^{-3} at 290 K; red vertical whiskers indicate their reported variability. The red dashed lines simply connect compounds to guide the eye. "n.d." = no k′ reported (IcdP).

https://doi.org/10.5194/egusphere-2025-6287
Preprint. Discussion started: 23 January 2026

4. Conclusion

This study demonstrates the development and evaluation of a TSOD adapted for UFP sampling. Under controlled laboratory conditions, the TSOD removed O_3 effectively for O_3 mixing ratios of up to 200 ppbV and constant relative humidity of 53%. The same was observed during a five days field campaign, with varying ambient O_3 mixing ratios (0–65 ppbV) and relative humidity (38–99 %). No significant particle losses were observed in the 10–100 nm and 10–1000 nm range across various flow rates, with relative average deviation of 5%, remaining within instrumental uncertainty.

Utilizing a dual-channel approach, we compared the impact of upstream O_3 removal prior to filter based analysis of mass concentrations of selected UFP-bound marker compounds of diverse chemical properties and of well-known interest in atmospheric studies. O_3-sensitive markers such as PAHs and 6PPD showed markable inter-channel differences: relative O_3-induced losses reached 15–46 % for higher molecular weight PAHs and up to 48 % for 6PPD. In contrast, 6PPDq concentrations increased in the O_3-exposed channel, consistent with in-situ formation from 6PPD. Quantitative comparison of absolute concentrations suggests a 6PPD to 6PPDq transformation of about 13 to 20 %, in agreement with previously reported laboratory yields. BOAs showed no inter-channel effect, implying that the TSOD did not induce a measurable change in particle reactivity or phase distribution of these semi-volatile species. Such change would need to be large enough to overcome analytical variability, which we do not observe.

Without an upstream O_3 denuder, systematic sampling artefacts occur: PAHs and 6PPD are systematically and significantly underestimated, while oxidation products such as 6PPDq are overestimated due to in-situ ozonolysis. Thus, O_3 removal is a methodological requirement for quantitative chemical UFP analysis. The TSOD meets the requirements by (i) efficiently scrubbing O_3 at atmospherically relevant mixing ratios, (ii) introducing no measurable particle loss across sizes from 10 nm to 1000 nm, and (iii) not perturbing the gas–particle partitioning of semi-volatile bOAs.

Data Availability

Data will be made available upon request.

Author contributions

EE: denuder design & preparation, laboratory and field deployment, measurements, chemical analysis, data processing and interpretation, and writing (original draft, review, editing).

AM, DB: DMS500 measurements, data analysis

NG: filter collection and writing (review and editing)

MS, RS, ACN: funding acquisition, conceptualization, supervision, and writing (review and editing)

Competing interests

The authors declare that they have no conflict of interest.

Acknowledgement

We thank the Bavarian Environment Agency (LfU) and the German Weather Service (DWD) for providing ozone and meteorological data.

This project is financed by the Bavarian State Ministry of the Environment and Consumer Protection. The article processing charges for this open-access publication were covered by the Forschungszentrum Jülich.

References

Abdel-Shafy, H. I., & Mansour, M. S. M. (2016). A review on polycyclic aromatic hydrocarbons: Source, environmental impact, effect on human health and remediation. *Egyptian Journal of Petroleum*, *25*(1), 107–123. https://doi.org/10.1016/j.ejpe.2015.03.011

Balducci, C., Cecinato, A., Paolini, V., Guerriero, E., Perilli, M., Romagnoli, P., Tortorella, C., Iacobellis, S., Giove, A., & Febo, A. (2018). Volatilization and oxidative artifacts of PM bound PAHs collected at low volume sampling (1): Laboratory and field evaluation. *Chemosphere*, *200*, 106–115. https://doi.org/10.1016/j.chemosphere.2018.02.090

Balmes, J. R., & Hansel, N. N. (2024). Tiny Particles, Big Health Impacts. *American Journal of Respiratory and Critical Care Medicine*, *210*(11), 1291–1292. https://doi.org/10.1164/rccm.202407-1476ED

Bedjanian, Y., & Nguyen, M. L. (2010). Kinetics of the reactions of soot surface-bound polycyclic aromatic hydrocarbons with O3. *Chemosphere*, *79*(4), 387–393. https://doi.org/10.1016/j.chemosphere.2010.02.009

Bell, M. L., Goldberg, R., Hogrefe, C., Kinney, P. L., Knowlton, K., Lynn, B., Rosenthal, J., Rosenzweig, C., & Patz, J. A. (2007). Climate change, ambient ozone, and health in 50 US cities. *Climatic Change*, *82*(1–2), 61–76. https://doi.org/10.1007/s10584-006-9166-7

Bouvier-Brown, N. C., Goldstein, A. H., Gilman, J. B., Kuster, W. C., & de Gouw, J. A. (2009). In-situ ambient quantification of monoterpenes, sesquiterpenes, and related oxygenated compounds during BEARPEX 2007: implications for gas- and particle-phase chemistry. *Atmospheric Chemistry and Physics*, *9*(15), 5505–5518. https://doi.org/10.5194/acp-9-5505-2009

Cataldo, F. (2019). Protection Mechanism of Rubbers from Ozone Attack. *Ozone: Science & Engineering*, *41*(4), 358–368. https://doi.org/10.1080/01919512.2018.1542518

Christoffersen, T. S., Hjorth, J., Horie, O., Jensen, N. R., Kotzias, D., Molander, L. L., Neeb, P., Ruppert, L., Winterhalter, R., Virkkula, A., Wirtz, K., & Larsen, B. R. (1998). cis-pinic acid, a possible precursor for organic aerosol formation from ozonolysis of α-pinene. *Atmospheric Environment*, *32*(10), 1657–1661. https://doi.org/10.1016/S1352-2310(97)00448-2

Cooper, O. R., Parrish, D. D., Ziemke, J., Balashov, N. V., Cupeiro, M., Galbally, I. E., Gilge, S., Horowitz, L., Jensen, N. R., Lamarque, J. F., Naik, V., Oltmans, S. J., Schwab, J., Shindell, D. T., Thompson, A. M., Thouret, V., Wang, Y., & Zbinden, R. M. (2014). Global distribution and trends of tropospheric ozone: An observation-based review. In *Elementa* (Vol. 2). BioOne. https://doi.org/10.12952/journal.elementa.000029

Das, A., Pantzke, J., Jeong, S., Hartner, E., Zimmermann, E. J., Gawlitta, N., Offer, S., Shukla, D., Huber, A., Rastak, N., Meščeriakovas, A., Ivleva, N. P., Kuhn, E., Binder, S., Gröger, T., Oeder, S., Delaval, M., Czech, H., Sippula, O., … Zimmermann, R. (2024). Generation, characterization, and toxicological assessment of reference ultrafine soot particles with different organic content for inhalation toxicological studies. *Science of The Total Environment*, *951*, 175727. https://doi.org/10.1016/j.scitotenv.2024.175727

Denjean, C., Formenti, P., Picquet-Varrault, B., Camredon, M., Pangui, E., Zapf, P., Katrib, Y., Giorio, C., Tapparo, A., Temime-Roussel, B., Monod, A., Aumont, B., & Doussin, J. F. (2015). Aging of secondary organic aerosol generated from the ozonolysis of α-pinene: effects of ozone, light and temperature. *Atmospheric Chemistry and Physics*, *15*(2), 883–897. https://doi.org/10.5194/acp-15-883-2015

Eckenberger, E., Mittereder, A., Gawlitta, N., Schnelle-Kreis, J., Sklorz, M., Brüggemann, D., Zimmermann, R., & Nölscher, A. C. (2025). Performance evaluation of four cascade impactors for airborne ultrafine-particle (UFP) collection: the influence of particle type, concentration, mass, and chemical nature. *Aerosol Research*, *3*(1), 45–64. https://doi.org/10.5194/ar-3-45-2025

Emberson, L. (2020). Effects of ozone on agriculture, forests and grasslands. *Philosophical Transactions of the Royal Society A: Mathematical, Physical and Engineering Sciences*, *378*(2183), 20190327. https://doi.org/10.1098/rsta.2019.0327

Ernle, L., Ringsdorf, M. A., & Williams, J. (2023). Influence of ozone and humidity on PTR-MS and GC-MS VOC measurements with and without a Na 2 S 2 O 3 ozone scrubber. *Atmospheric Measurement Techniques*, *16*(5), 1179–1194. https://doi.org/10.5194/amt-16-1179-2023

European Committee for Standardization (CEN). (2008). *EN 15549:2008 – Air quality — Standard method for the measurement of the concentration of benzo[a]pyrene and other polycyclic aromatic hydrocarbons in ambient air*.

Fick, J., Pommer, L., Andersson, B., & Nilsson, C. (2001). Ozone Removal in the Sampling of Parts per Billion Levels of Terpenoid Compounds: An Evaluation of Different Scrubber Materials. *Environmental Science & Technology*, *35*(7), 1458–1462. https://doi.org/10.1021/es0001456

Gaudel, A., Cooper, O. R., Ancellet, G., Barret, B., Boynard, A., Burrows, J. P., Clerbaux, C., Coheur, P.-F., Cuesta, J., Cuevas, E., Doniki, S., Dufour, G., Ebojie, F., Foret, G., Garcia, O., Granados-Muñoz, M. J., Hannigan, J. W., Hase, F., Hassler, B., … Ziemke, J. (2018). Tropospheric Ozone Assessment Report: Present-day distribution and trends of tropospheric ozone relevant to climate and global atmospheric chemistry model evaluation. *Elementa: Science of the Anthropocene*, *6*. https://doi.org/10.1525/elementa.291

https://doi.org/10.5194/egusphere-2025-6287
Preprint. Discussion started: 23 January 2026

Grosjean, D. (1992). In situ organic aerosol formation during a smog episode: Estimated production and chemical functionality. *Atmospheric Environment. Part A. General Topics*, *26*(6), 953–963. https://doi.org/10.1016/0960-1686(92)90027-I

Haddad, P., Jeong, H., Kappeler, R., Altug, H., Andersen, Z. J., Bergmann, M., Boogaard, H., Kutlar, M. J., Lim, Y. H., Loft, S., Pohl, T., & Hoffmann, B. (2024). Systematic review on health effects of long-term exposure to UFP. *ISEE Conference Abstracts*, *2024*(1). https://doi.org/10.1289/isee.2024.0574

Hellén, H., Kuronen, P., & Hakola, H. (2012). Heated stainless steel tube for ozone removal in the ambient air measurements of mono- and sesquiterpenes. *Atmospheric Environment*, *57*, 35–40. https://doi.org/10.1016/j.atmosenv.2012.04.019

Helmig, D. (1997). Ozone removal techniques in the sampling of atmospheric volatile organic trace gases. *Atmospheric Environment*, *31*(21), 3635–3651. https://doi.org/10.1016/S1352-2310(97)00144-1

Ho, S. S. H., Ip, H. S. S., Ho, K. F., Dai, W.-T., Cao, J., & Ng, L. P. T. (2013). Technical Note: Concerns on the Use of Ozone Scrubbers for Gaseous Carbonyl Measurement by DNPH-Coated Silica Gel Cartridge. *Aerosol and Air Quality Research*, *13*(4), 1151–1160. https://doi.org/10.4209/aaqr.2012.11.0313

Hu, X., Zhao, H. N., Tian, Z., Peter, K. T., Dodd, M. C., & Kolodziej, E. P. (2022). Transformation Product Formation upon Heterogeneous Ozonation of the Tire Rubber Antioxidant 6PPD (*N* -(1,3-dimethylbutyl)- *N* ′-phenyl- *p* -phenylenediamine). *Environmental Science & Technology Letters*, *9*(5), 413–419. https://doi.org/10.1021/acs.estlett.2c00187

Ji, Z., Zhang, N., Huang, C., Duan, X., Ren, D., & Huo, Z. (2024). The Degradation of Polycyclic Aromatic Hydrocarbons (PAHs) by Ozone-Based Advanced Oxidation Processes: A Review. *Ozone: Science & Engineering*, *46*(1), 26–42. https://doi.org/10.1080/01919512.2023.2192751

Koppmann, R., Johnen, F. J., Khedim, A., Rudolph, J., Wedel, A., & Wiards, B. (1995). The influence of ozone on light nonmethane hydrocarbons during cryogenic preconcentration. *Journal of Geophysical Research: Atmospheres*, *100*(D6), 11383–11391. https://doi.org/10.1029/95JD00561

Kristensen, K., Bilde, M., Aalto, P. P., Petäjä, T., & Glasius, M. (2016). Denuder/filter sampling of organic acids and organosulfates at urban and boreal forest sites: Gas/particle distribution and possible sampling artifacts. *Atmospheric Environment*, *130*, 36–53. https://doi.org/10.1016/j.atmosenv.2015.10.046

Kristensen, K., Watne, Å. K., Hammes, J., Lutz, A., Petäjä, T., Hallquist, M., Bilde, M., & Glasius, M. (2016). High-Molecular Weight Dimer Esters Are Major Products in Aerosols from α-Pinene Ozonolysis and the Boreal Forest. *Environmental Science & Technology Letters*, *3*(8), 280–285. https://doi.org/10.1021/acs.estlett.6b00152

Kuwabara, H., Sekiguchi, K., Sankoda, K., Sakurai, K., Yamaguchi, R., Furuuchi, M., & Hata, M. (2016). Evaluation of Artifacts Generated during Collection of Ultrafine Particles Using an Inertial Filter Sampler. *Aerosol and Air Quality Research*, *16*(12), 3063–3074. https://doi.org/10.4209/aaqr.2015.12.0679

Kwamena, N.-O. A., Clarke, J. P., Kahan, T. F., Diamond, M. L., & Donaldson, D. J. (2007). Assessing the importance of heterogeneous reactions of polycyclic aromatic hydrocarbons in the urban atmosphere using the Multimedia Urban Model. *Atmospheric Environment*, *41*(1), 37–50. https://doi.org/10.1016/j.atmosenv.2006.08.016

https://doi.org/10.5194/egusphere-2025-6287
Preprint. Discussion started: 23 January 2026

Kwon, H.-S., Ryu, M. H., & Carlsten, C. (2020). Ultrafine particles: unique physicochemical properties relevant to health and disease. *Experimental & Molecular Medicine*, *52*(3), 318–328. https://doi.org/10.1038/s12276-020-0405-1

Li, Q.-Q., Guo, Y.-T., Yang, J.-Y., & Liang, C.-S. (2023). Review on main sources and impacts of urban ultrafine particles: Traffic emissions, nucleation, and climate modulation. *Atmospheric Environment: X*, *19*, 100221. https://doi.org/10.1016/j.aeaoa.2023.100221

Liffick, G. L. (1970). *An Investigation of the Removal of Ozone by Activated Charcoal*. Oregon State University.

Liu, K., Duan, F., He, K., Ma, Y., & Cheng, Y. (2014). Investigation on sampling artifacts of particle associated PAHs using ozone denuder systems. *Frontiers of Environmental Science & Engineering*, *8*(2), 284–292. https://doi.org/10.1007/s11783-013-0555-7

Liu, Y., Sklorz, M., Schnelle-Kreis, J., Orasche, J., Ferge, T., Kettrup, A., & Zimmermann, R. (2006). Oxidant denuder sampling for analysis of polycyclic aromatic hydrocarbons and their oxygenated derivates in ambient aerosol: Evaluation of sampling artefact. *Chemosphere*, *62*(11), 1889–1898. https://doi.org/10.1016/j.chemosphere.2005.07.049

Marval, J., & Tronville, P. (2022). Ultrafine particles: A review about their health effects, presence, generation, and measurement in indoor environments. *Building and Environment*, *216*, 108992. https://doi.org/10.1016/j.buildenv.2022.108992

Monks, P. S., Archibald, A. T., Colette, A., Cooper, O., Coyle, M., Derwent, R., Fowler, D., Granier, C., Law, K. S., Mills, G. E., Stevenson, D. S., Tarasova, O., Thouret, V., von Schneidemesser, E., Sommariva, R., Wild, O., & Williams, M. L. (2015). Tropospheric ozone and its precursors from the urban to the global scale from air quality to short-lived climate forcer. *Atmospheric Chemistry and Physics*, *15*(15), 8889–8973. https://doi.org/10.5194/acp-15-8889-2015

Mutzel, A., Rodigast, M., Iinuma, Y., Böge, O., & Herrmann, H. (2016). Monoterpene SOA – Contribution of first-generation oxidation products to formation and chemical composition. *Atmospheric Environment*, *130*, 136–144. https://doi.org/10.1016/j.atmosenv.2015.10.080

Oberdörster, G., Ferin, J., Gelein, R., Soderholm, S. C., & Finkelstein, J. (1992). Role of the alveolar macrophage in lung injury: studies with ultrafine particles. *Environmental Health Perspectives*, *97*, 193–199. https://doi.org/10.1289/ehp.97-1519541

Ofner, J., Krüger, H. U., Grothe, H., Schmitt-Kopplin, P., Whitmore, K., & Zetzsch, C. (2011). Physico-chemical characterization of SOA derived from catechol and guaiacol - A model substance for the aromatic fraction of atmospheric HULIS. *Atmospheric Chemistry and Physics*, *11*(1), 1–15. https://doi.org/10.5194/acp-11-1-2011

Pantzke, J., Das, A., Zimmermann, E. J., Offer, S., Jeong, S., Delaval, M. N., Schnelle-Kreis, J., Sklorz, M., Bucchianico, S. Di, & Zimmermann, R. (2023). 68 On the Role of Chemical Identity over the size of Model Ultrafine Particles Driven (geno)-Toxicity. *Annals of Work Exposures and Health*, *67*(Supplement_1), i93–i93. https://doi.org/10.1093/annweh/wxac087.227

Pollmann, J., Ortega, J., & Helmig, D. (2005). Analysis of Atmospheric Sesquiterpenes: Sampling Losses and Mitigation of Ozone Interferences. *Environmental Science & Technology*, *39*(24), 9620–9629. https://doi.org/10.1021/es050440w

Pöschl, U., Letzel, T., Schauer, C., & Niessner, R. (2001). Interaction of Ozone and Water Vapor with Spark Discharge Soot Aerosol Particles Coated with Benzo[*a*]pyrene: O 3 and H 2 O Adsorption, Benzo[*a*]pyrene Degradation, and Atmospheric Implications. *The Journal of Physical Chemistry A*, *105*(16), 4029–4041. https://doi.org/10.1021/jp004137n

Prather, M. J., & Zhu, X. (2024). Lifetimes and timescales of tropospheric ozone. *Elem Sci Anth*, *12*(1). https://doi.org/10.1525/elementa.2023.00112

RAVINDRA, K., SOKHI, R., & VANGRIEKEN, R. (2008). Atmospheric polycyclic aromatic hydrocarbons: Source attribution, emission factors and regulation. *Atmospheric Environment*, *42*(13), 2895–2921. https://doi.org/10.1016/j.atmosenv.2007.12.010

Rossomme, E., Hart-Cooper, W. M., Orts, W. J., McMahan, C. M., & Head-Gordon, M. (2023). Computational Studies of Rubber Ozonation Explain the Effectiveness of 6PPD as an Antidegradant and the Mechanism of Its Quinone Formation. *Environmental Science & Technology*, *57*(13), 5216–5230. https://doi.org/10.1021/acs.est.2c08717

Rynek, R., Mayer, T., & Borsdorf, H. (2025). Enhancing forest air sampling using a novel reusable ozone filter design. *Atmospheric Measurement Techniques*, *18*(17), 4103–4117. https://doi.org/10.5194/amt-18-4103-2025

Schraufnagel, D. E. (2020). The health effects of ultrafine particles. *Experimental & Molecular Medicine*, *52*(3), 311–317. https://doi.org/10.1038/s12276-020-0403-3

Shiraiwa, M., Ammann, M., Koop, T., & Pöschl, U. (2011). Gas uptake and chemical aging of semisolid organic aerosol particles. *Proceedings of the National Academy of Sciences*, *108*(27), 11003–11008. https://doi.org/10.1073/pnas.1103045108

Subramanian, R., Khlystov, A. Y., Cabada, J. C., & Robinson, A. L. (2004). Positive and Negative Artifacts in Particulate Organic Carbon Measurements with Denuded and Undenuded Sampler Configurations Special Issue of *Aerosol Science and Technology* on Findings from the Fine Particulate Matter Supersites Program. *Aerosol Science and Technology*, *38*(sup1), 27–48. https://doi.org/10.1080/02786820390229354

Takizawa, M., Okuwaki, A., & Okabe, T. (1973). The Chemical Behavior of Low Valence Sulfur Compounds. VIII. The Oxidation of Sodium Thiosulfate with Ozone. *Bulletin of the Chemical Society of Japan*, *46*(12), 3785–3789. https://doi.org/10.1246/bcsj.46.3785

Van Vaeck, L., & Van Cauwenberghe, K. (1984). Conversion of polycyclic aromatic hydrocarbons on diesel particulate matter upon exposure to ppm levels of ozone. *Atmospheric Environment (1967)*, *18*(2), 323–328. https://doi.org/10.1016/0004-6981(84)90106-9

WHO global air quality guidelines. Particulate matter (PM2.5 and PM10), ozone, nitrogen dioxide, sulfur dioxide and carbon monoxide. (n.d.).

Williams, E. L., & Grosjean, D. (1990). Removal of atmospheric oxidants with annular denuders. *Environmental Science & Technology*, *24*(6), 811–814.

https://doi.org/10.5194/egusphere-2025-6287
Preprint. Discussion started: 23 January 2026

Yatavelli, R. L. N., Lopez-Hilfiker, F., Wargo, J. D., Kimmel, J. R., Cubison, M. J., Bertram, T. H., Jimenez, J. L., Gonin, M., Worsnop, D. R., & Thornton, J. A. (2012). A Chemical Ionization High-Resolution Time-of-Flight Mass Spectrometer Coupled to a Micro Orifice Volatilization Impactor (MOVI-HRToF-CIMS) for Analysis of Gas and Particle-Phase Organic Species. *Aerosol Science and Technology*, *46*(12), 1313–1327. https://doi.org/10.1080/02786826.2012.712236

Yatavelli, R. L. N., Stark, H., Thompson, S. L., Kimmel, J. R., Cubison, M. J., Day, D. A., Campuzano-Jost, P., Palm, B. B., Hodzic, A., Thornton, J. A., Jayne, J. T., Worsnop, D. R., & Jimenez, J. L. (2014). Semicontinuous measurements of gas–particle partitioning of organic acids in a ponderosa pine forest using a MOVI-HRToF-CIMS. *Atmospheric Chemistry and Physics*, *14*(3), 1527–1546. https://doi.org/10.5194/acp-14-1527-2014

Young, P. J., Archibald, A. T., Bowman, K. W., Lamarque, J.-F., Naik, V., Stevenson, D. S., Tilmes, S., Voulgarakis, A., Wild, O., Bergmann, D., Cameron-Smith, P., Cionni, I., Collins, W. J., Dalsøren, S. B., Doherty, R. M., Eyring, V., Faluvegi, G., Horowitz, L. W., Josse, B., … Zeng, G. (2013). Pre-industrial to end 21st century projections of tropospheric ozone from the Atmospheric Chemistry and Climate Model Intercomparison Project (ACCMIP). *Atmospheric Chemistry and Physics*, *13*(4), 2063–2090. https://doi.org/10.5194/acp-13-2063-2013

Yu, J., Griffin, R. J., Cocker, D. R., Flagan, R. C., Seinfeld, J. H., & Blanchard, P. (1999). Observation of gaseous and particulate products of monoterpene oxidation in forest atmospheres. *Geophysical Research Letters*, *26*(8), 1145–1148. https://doi.org/10.1029/1999GL900169

Zhang, J. (Jim), Wei, Y., & Fang, Z. (2019). Ozone Pollution: A Major Health Hazard Worldwide. *Frontiers in Immunology*, *10*. https://doi.org/10.3389/fimmu.2019.02518

Zhao, H. N., Hu, X., Tian, Z., Gonzalez, M., Rideout, C. A., Peter, K. T., Dodd, M. C., & Kolodziej, E. P. (2023). Transformation Products of Tire Rubber Antioxidant 6PPD in Heterogeneous Gas-Phase Ozonation: Identification and Environmental Occurrence. *Environmental Science & Technology*, *57*(14), 5621–5632. https://doi.org/10.1021/acs.est.2c08690

Zhao, Z., Hao, J., LI, J., & WU, S. (2008). Second organic aerosol formation from the ozonolysis of α-pinene in the presence of dry submicron ammonium sulfate aerosol. *Journal of Environmental Sciences*, *20*(10), 1183–1188. https://doi.org/10.1016/S1001-0742(08)62207-X

Zhou, S., Hwang, B. C. H., Lakey, P. S. J., Zuend, A., Abbatt, J. P. D., & Shiraiwa, M. (2019). Multiphase reactivity of polycyclic aromatic hydrocarbons is driven by phase separation and diffusion limitations. *Proceedings of the National Academy of Sciences*, *116*(24), 11658–11663. https://doi.org/10.1073/pnas.1902517116